

Structural characterization of polycrystalline Cd–Te–In films

M. Zapata-Torres

Instituto de Física de São Carlos–USP, Caixa Postal 369, CEP 13560-940, São Carlos, SP, Brazil and CICATA–IPN Unidad Altamira, Km. 14.5 Carretera Tampico-Puerto Industrial Altamira, 86900 Altamira, Tamps., México

R. Castro-Rodríguez^{a)}

Departamento de Física Aplicada, CINVESTAV–IPN, Unidad Mérida, A.P. 73, Cordemex, Mérida Yucatan 97310, México

A. Martel

CICATA–IPN Unidad Altamira, Km. 14.5 Carretera Tampico-Puerto Industrial Altamira, 86900 Altamira, Tamps., México and Facultad de Física, Universidad de La Habana, San Lázaro y L. Vedado, A.P. 6426, 10400 La Habana, Cuba

Y. P. Mascarenhas and J. Guevara

Instituto de Física de São Carlos–USP, Caixa Postal 369, CEP 13560-940, São Carlos, SP, Brazil

M. Melendez-Lira

Departamento de Física, CINVESTAV–IPN, Apartado Postal 14-740, México D. F. 07000, México

J. L. Peña

CICATA–IPN Unidad Altamira, Km. 14.5 Carretera Tampico-Puerto Industrial Altamira, 86900 Altamira, Tamps., México and Departamento de Aplicada, CINVESTAV–IPN, Unidad Mérida, A.P. 73, Cordemex, Mérida Yucatan 97310, México

(Received 6 April 2000; accepted 11 September 2000)

Polycrystalline Cd–Te–In films have been grown on glass substrates by close-spaced vapor transport combined with a free evaporation technique and the stoichiometric, structural and electrical properties were investigated as functions of In_2Te_3 concentration added in solid solution into the CdTe structure during In incorporation. Indium was introduced by evaporation during film preparation and the incorporation was controlled by the temperature of the In source. The composition of the films was investigated by Auger electron spectroscopy, showing that, when In concentration increases the Cd concentration decreases they have a similar value (≈ 22 at. %) at about 750 °C In source temperature. The dark resistivity decreased monotonically four orders of magnitude with the In_2Te_3 concentration and reached a minimum point. From the structural characterization employed it was shown that the In atoms are incorporated in two ways: (I) for as low-In concentration, the In atoms substitute the Cd atoms, decreasing the resistivity; and (II) for high-In concentration, the In atoms form with the CdTe a solid solution like $(\text{CdTe})_{1-x}(\text{In}_2\text{Te}_3)_x$. The x-ray spectra were calculated for In source temperatures of 550 and 750 °C using structure refinement by the Rietveld method and general structure analysis system software. A good agreement between experimental and calculated spectra was found for both temperatures. © 2001 American Vacuum Society. [DOI: 10.1116/1.1322643]

I. INTRODUCTION

Semiconductor thin films have specific importance and interest for possible applications to optoelectronic devices such as smart pixel arrays. Therefore, the search for and development of preparation methods which lead to films with sophisticated optical qualities in easily controllable ways have attracted growing interest for both research and technical applications. CdTe is a II–VI semiconductor compound which has been used in several optoelectronic devices such as infrared and gamma radiation detectors, solar cells, etc. The energy of its band gap of 1.5 eV,¹ located at the maximum of the solar energy density incident on the Earth's surface, makes this material very suitable for photovoltaic applications. The incorporation of In atoms at low concen-

tration into doped CdTe monolayers has been achieved by photoassisted molecular beam epitaxy.² The effects of heavy doping in CdTe due to high In concentrations has been observed in CdTe polycrystalline films obtained by thermal coevaporation³ and cosputtering⁴ of CdTe and In. In order to explain all the compounds formed by mixing CdTe and In, they are described using the phase diagram of the CdTe– In_2Te_3 system⁵ from the In_2Te_3 added in solid solution into the CdTe structure as $(\text{CdTe})_{1-x}(\text{In}_2\text{Te}_3)_x$ during the incorporation of In. In this system the CdTe has a zinc blende structure (α phase) with lattice parameter $a = 6.481$ Å. As In_2Te_3 is added to the lattice parameter is decreased, and several ternary compounds have been reported: β phase with a chalcopyrite-like structure and $x = 0.42$ – 0.72 is a very wide phase field to call it CIT (particularly the ternary compound CdIn_2Te_4 is formed at x

^{a)}Electronic mail: romano@mda.cinvestav.mx

$=0.5$), $\text{CdIn}_8\text{Te}_{13}$ (δ phase) with a cubic structure at $x = 0.8$, and $\text{CdIn}_{30}\text{Te}_{46}$ (γ phase) with a cubic structure at approximately $x = 0.94$. This system has been investigated by melting of different concentration of these elements.⁵⁻⁷

Close-spaced vapor transport combined with free evaporation (CSVTE) is a convenient method by which to grow ternary materials because it is possible to control the temperatures of different compounds separately.⁸ It is also cost effective since it can operate at atmospheric pressure under inert gas and uses moderate temperatures; its operation is simple, and films are compact, with few voids. In this work the chemical composition and structural and electrical properties of Cd–Te–In films as a function of In_2Te_3 concentration are presented in order to explain the mechanisms of incorporation of In atoms into the CdTe structure.

II. SAMPLE PREPARATION

All films were prepared in a conventional vacuum evaporation system evacuated by an oil-diffusion pump with a liquid-nitrogen trap, capable of obtaining a background pressure of 10^{-6} Torr. The pressure during evaporation was below 10^{-5} Torr. To obtain Cd–Te–In films we used the deposition technique previously reported by two of the authors⁹ consisting of CSVTE combined with free evaporation. In our experiments we used high-purity Balzers metallic indium (99.999 at. % pure). The CdTe powder (99.99 at. % pure Balzers) sublimates at a temperature of 500 °C during the growth process, while the In source was varied between 500 and 800 °C, in steps of 25 °C, to achieve different In concentrations. Corning 7059 glass slides were used as substrates. We kept the substrate temperature at 400 °C and the deposition time of 10 min fixed. The control gas used during film growth was Matheson argon 99.999 at. %.

III. MEASUREMENT EQUIPMENT

Compositional measurements were performed by the Auger electron spectroscopy (AES) technique with an ESCA/SAM Perkin Elmer PHI 560 equipped with a double pass cylindrical mirror analyzer, with a base pressure of $\sim 2 \times 10^{-9}$ Torr. AES signals were obtained in differential mode using a 3 keV, 0.2 μA electron beam incident at 45° to the surface normal. AES profiles were obtained with an Ar^+ beam with energy of 4 keV and current density of 0.36 $\mu\text{A cm}^{-2}$, yielding a sputtering rate of about 10 nm/min. The calibration of the sensitivity factor of Auger data was made using stoichiometric CdTe. X-ray diffraction (XRD) measurements in a grazing incidence geometry with 0.5° beam inclination were done under $\text{Cu K}\alpha$ radiation at 40 kV with 35 mA and an aperture diaphragm of 0.2° using a Siemens D5000 x-ray diffractometer with monochromatic radiation ($\lambda = 1.5418 \text{ \AA}$). The films were carefully mounted so there was no misalignment. The scanning step of the goniometer was 0.01° with a counting time of 10 s. Scattered radiation passed through an arrangement of horizontal slits to the detector. The dark electrical conductivity of the films was measured at room temperature using the van der Pauw method.

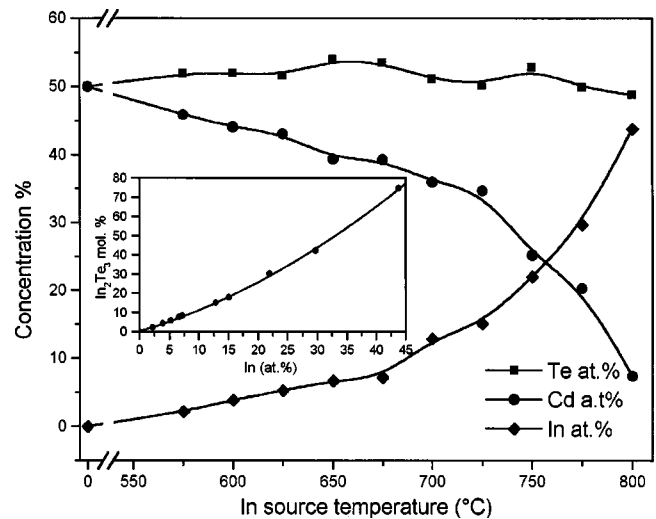


FIG. 1. Atomic composition of the Cd–Te–In films determined by AES vs indium source temperature. The inset shows the relationship between the In at. % and the mol % of In_2Te_3 in CdTe.

Electrical contacts were made with metallic indium previously evaporated onto the film, and are heated 50 °C over the melting point of indium for 5 min under inert atmosphere.

IV. RESULTS AND DISCUSSION

The surfaces of the films were smooth and slightly grayish. All the films firmly adhered to the substrate. The films are polycrystalline, with uniform thickness (around 25 μm). The relative atomic concentration values for all films were determined by AES. Figure 1 shows the relation between atomic concentrations of the films and the In temperature source. From to 550 °C, the In concentration increases monotonically and the Cd concentration decreases while the Te concentration remains constant. Then, the atomic concentration of the In and Cd shows a similar value (≈ 22 at. %) at about 750 °C. From 700 °C a mixture of the elements Cd, Te and In as a solid solution like $(\text{CdTe})_{1-x}(\text{In}_2\text{Te}_3)_x$ is formed, as a result of the In_2Te_3 added in solid solution into the CdTe structure. The molar fraction of the In_2Te_3 in the above solution was calculated from the AES data, and the result is shown in the inset. This will be used in the following discussions. On the other hand, the relation between the dark resistivity of the films at 20 °C and the molar fraction of the In_2Te_3 is shown in Fig. 2. The dark resistivity first decreased monotonically four orders of magnitude with the In_2Te_3 molar fraction and reached a minimum point. Afterwards, the resistivity increased to a maximum point, after that it showed a saturation tendency. Similar behavior was found in previous work¹⁰ from a measurement of thermal diffusivity.

To explain the characteristics observed in both Figs. 1 and 2, we analyzed the film structure in detail using x-ray diffraction analysis. Indium can be doped into Cd vacancies of CdTe crystallites substitutionally and can act as a donor during the low-In concentration stage (500–625 °C). The decrease in the film resistivity at low-In concentration stage is thought to be due to this effect. The resistivity increase over

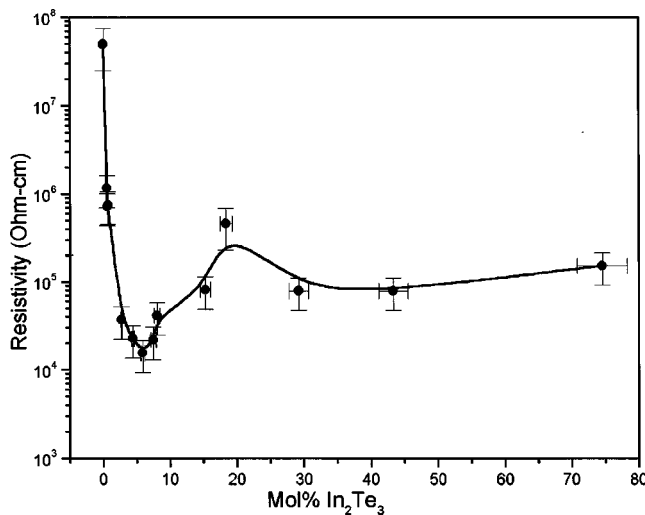


FIG. 2. Dark electrical resistivity of the Cd-Te-In films as a function of In_2Te_3 mol % in CdTe.

the peak may be that the lattice becomes greatly distorted because the radius of the In^{3+} ion (0.92 Å) is smaller than the Cd^{2+} ion radius (1.03 Å), and the distorted lattice may enhance the electron scattering and decrease the mobility. Therefore, a CdTe lattice doped with substitutional In atoms may shrink and become distorted. This can clearly be seen in Fig. 3. Figure 3 displays the normalized three-dimensional (3D) x-ray diffraction pattern showing the evolution of the present structural phases in our samples, from 0 to about 10 mol % In_2Te_3 . The films present α phase and the only observed effect is a decrease of the lattice parameter. For In_2Te_3 concentration greater than 10 mol % progressive shifting and deformation of the [111] CdTe peak can be observed and the presence of another peak, which tends towards the position of the CdIn_2Te_4 [112] peak. At about 30 mol % of In_2Te_3 both of the peaks are well defined.

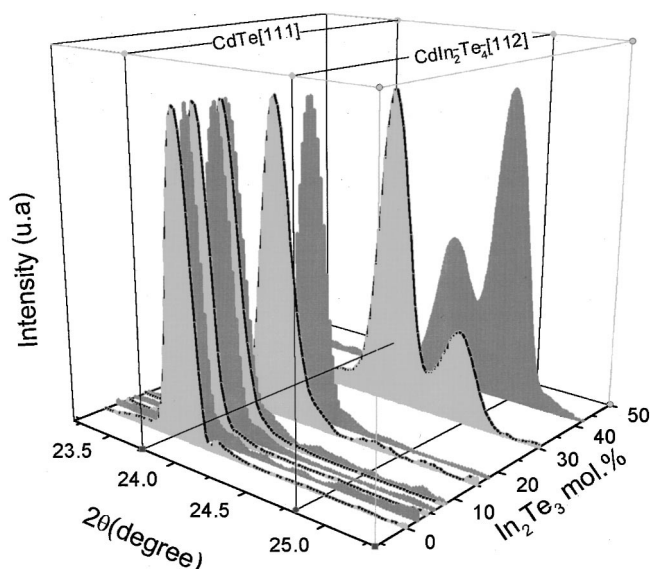


FIG. 3. Three-dimensional normalized x-ray diffraction patterns plotted as a function of the In_2Te_3 mol % in CdTe.

Such behavior is related to the presence of the β phase from 10 to 15 mol % of In_2Te_3 . The above results agree very well with the phase diagram for the CdTe- In_2Te_3 system reported by Thomassen *et al.*⁵ According to this diagram, for concentrations below 10 mol %, only the α phase can be present. In Cd deficient polycrystalline films like CdTe films, the In can occupy the Cd vacancies in this mol % region. From 10 to 42 mol % In_2Te_3 the α and β phases have to be present. Thus in this region the films are a solid solution of the above phases. Besides the above, we did not find the CdTe [111] peak in the x-ray diffraction pattern of the film grown at In source temperature of 800 °C. It is due to the mol % In_2Te_3 of this film (75 mol %) which lies in the region of the phase diagram where the α phase cannot be present.

Mixtures of a II-VI compound like CdTe and III-VI compound like In_2Te_3 form extended regions of solid solutions. As both components crystallize in the zinc blende lattice, one would expect that the solid solutions are also of zinc blende type. However, because of the stoichiometric ratio of 2:3 for In:Te, one third of the sites in the cation sublattice of In_2Te_3 are vacant. The concentration of these structural vacancies in the solid solutions decreases with an increasing amount of the II-VI component. In the solid solution the content of vacancies will be randomly distributed. The structural vacancies in the cation sublattice, which are caused by the different valences of Cd^{2+} and In^{3+} ions, are characteristic for all solid solutions of II-VI and III-VI compounds.

In fact, the ternary compound $(\text{CdTe})_{1-x}(\text{In}_2\text{Te}_3)_x$ could be written as $\text{Cd}_{1-x}\text{In}_{(2/3)x}\text{Te}$, and the relation between the lattice parameter and the molar fraction of In_2Te_3 in CdTe has been reported by Weitz and Leute⁷ as

$$a(x)(\text{\AA}) = 6.484 - 0.336x \quad (0 < x < 0.7), \quad (1)$$

$$a^*(x)(\text{\AA}) = 6.120 + 0.455x - 0.413x^2 \quad (0.7 < x < 1), \quad (2)$$

where a is a cubic lattice constant, a^* is a pseudocubic lattice constant, x is a molar fraction of In_2Te_3 in CdTe and from these results we calculated the lattice parameter as a function of the cation vacancies in the solid solutions. Using $\text{Cd}_{1-x}\text{In}_{(2/3)x}\text{Te}$, we can write the cation vacancies (CV) as $\text{CV} = 1 - (1-x) - (2/3)x = (1/3)x$ where 1 represents the total cation sites, $(1-x)$ are the sites occupied by Cd and $(2/3)x$ are the sites occupied by In. The lattice parameter as a function of CV can be written, with substitution in Eqs. (1) and (2), as

$$a(\text{CV})(\text{\AA}) = 6.484 - 1.008 \text{ CV} \quad (0 < \text{CV} < 0.233), \quad (3)$$

$$a^*(\text{CV})(\text{\AA}) = 6.120 + 1.365 \text{ CV} - 3.717(\text{CV})^2 \quad (0.233 < \text{CV} < 0.333). \quad (4)$$

A plot of these theoretical results and the experimental film data are shown in Fig. 4. The theoretical curve and the experiment, in general, agree well. However, we considered it necessary to make a distinction in the region corresponding to the 10 mol % In_2Te_3 value, below which only the α phase is present. This is shown in the inset of Fig. 4. One can see a

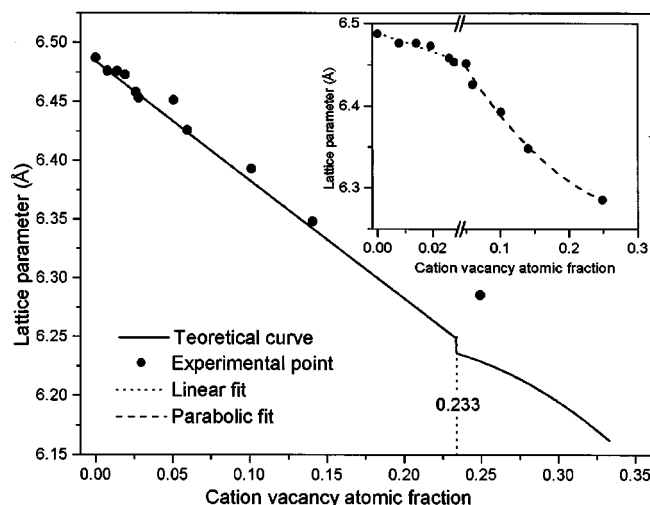


FIG. 4. Lattice parameter as a function of cation vacancy in the solid solution $(\text{CdTe})_{1-x}(\text{In}_2\text{Te}_3)_x$.

linear region corresponding to occupation of the Cd vacancies by In and a parabolic region corresponding to the solid solution. The fitting of the regions is

$$a(\text{CV})(\text{\AA}) = 6.48797 - 1.10919 \text{ CV} \quad (0 < \text{CV} < 0.028), \quad (5)$$

$$a(\text{CV})(\text{\AA}) = 6.51452 - 1.48079 \text{ CV} + 2.24766 \text{ CV}^2 \quad (0.028 < \text{CV} < 0.25). \quad (6)$$

The break region of the plot corresponds to the 10 mol % In_2Te_3 .

To explain the results observed in Fig. 4, we had supposed from our x-ray results that the In incorporation into CdTe was made in two ways: (I) for low-In concentration, where the In atoms substitute the vacancies of Cd atoms, and (II) for high-In concentration, where the In atoms form with the CdTe as a solid solution $(\text{CdTe})_{1-x}(\text{In}_2\text{Te}_3)_x$.

In order to confirm our observation, two representative samples, one for each incorporation mechanism [(I) and (II)], were selected to perform structure refinement by the Rietveld method using the general structure analysis system (GSAS) program.¹¹ The structures were refined with the space group $F-43M$. The refined instrumental and structural parameters were peak shape (using a pseudo-Voigt peak profile function), scale factor, background, unit cell parameters, position parameters, isotropic thermal parameters and preferred orientation. We introduced the effect of cation vacancies into the site occupancy factors of the atoms and fixed them. The final refinement cycles yielded conventional reliability factors of $R_{\text{Bragg}} = 9.8\%$ and 9.0% , which give irrefutable evidence of our structural model.

The plot of observed and calculated x-ray diffraction patterns is shown in Fig. 5 for the sample with indium source temperature of 550°C . The curves are vertically shifted. This plot corresponds to the sample of mechanism (I). In this case

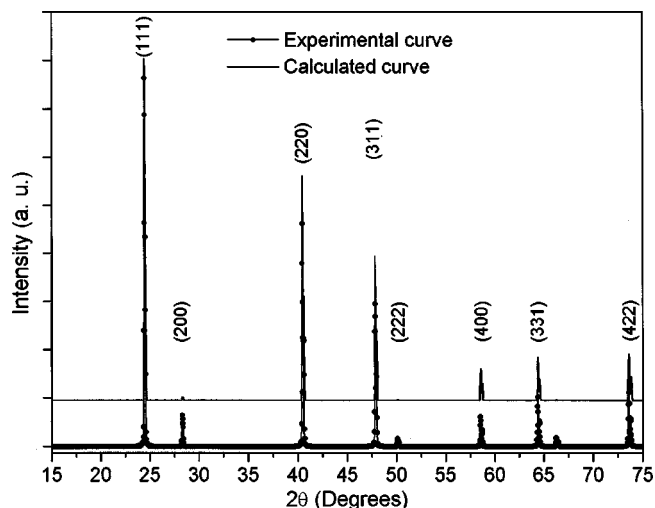


FIG. 5. Rietveld method refined profile of x-ray diffraction data for a sample with an indium source temperature of 550°C .

we supposed that the In atoms substitute for the Cd atoms. We can see the peaks related to the (111), (220), (311), (400), (331), and (422) planes.

Figure 6 shows x-ray diffraction for the sample with In source temperature of 750°C . We can see the plot corresponding to mechanism II. The curves are vertically shifted. In this refinement we supposed that two In atoms substituted for three Cd atoms, yielding one vacancy. By calculating the lattice constant, we obtained the amount of vacancies present in the solid solution (using Fig. 4). We can see additional peaks related to the (200), (222), and (420) planes. This could be due to the fact that an increase of vacancies increases the relative intensities of these peaks, and to a preferential orientation effect.

In addition to the above models, another model may be considered: many In atoms may deposit at grain boundaries or upon the surface of the film after growth; however, if this

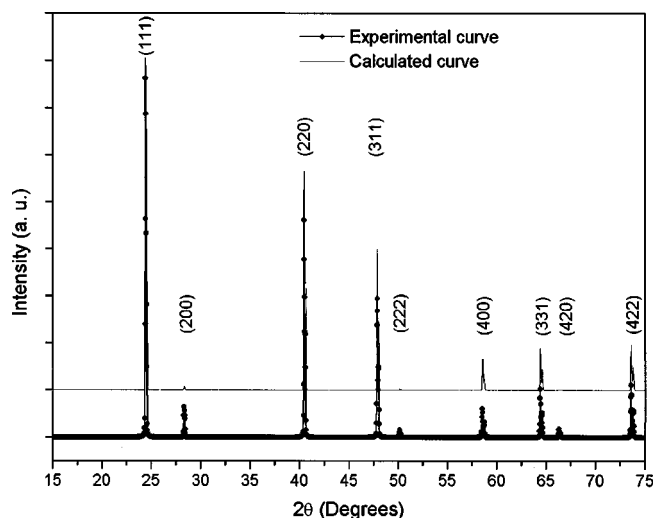


FIG. 6. Rietveld method refined profile of x-ray diffraction data for a sample with an indium source temperature of 750°C .

is true, the larger peaks corresponding to In should appear in the x-ray-diffraction pattern shown in Fig. 3, and these peaks were not detected in our films as can be seen in Fig. 3.

V. CONCLUSIONS

In summary, all the results obtained from the structural characterization employed indicated that the In atoms are incorporated in two ways: (I) for as low-In concentration, the In atoms substitute for Cd atoms, decreasing the resistivity by four orders of magnitude; and (II) for high-In concentration, where the In atoms form with the CdTe a solid solution like $(\text{CdTe})_{1-x}(\text{In}_2\text{Te}_3)_x$. All the results agree well with the phase diagram for the CdTe–In₂Te₃ system.

ACKNOWLEDGMENTS

The authors would like to thank Oswaldo Gómez, Mario Herrera, Victor Rejón, Wilian Cauich, Jose A. L. da Rocha, Jose G. Catarino, and Roberto Sánchez for technical assistance and CONACyT (Mexico) for financial support under Project Nos. 2367PE9509, 5372E, and F586-E9403. One of

the authors (M.Z.-T. acknowledges financial support of CONACyT (Mexico) for postdoctoral training at the IFSC-USP Institute and a second author (A.M. acknowledges COFAA-IPN for financial support.

¹D. de Novel, Philips Res. Rep. **14**, 361 (1959).

²R. N. Bicknell, N. C. Giles, and J. F. Schetzina, Appl. Phys. Lett. **49**, 1095 (1986).

³T. Hayashi, T. Suzuki, and Y. Ema, J. Appl. Phys. **27**, 1626 (1988).

⁴R. Ramírez-Bom, R. Nuñez-López, F. J. Espinoza-Beltrán, O. Zelaya-Angel, and J. González-Hernández, J. Phys. Chem. Solids **58**, 807 (1997).

⁵L. Thomassen, D. R. Mason, G. D. Rose, J. C. Sarace, and G. A. Schmitt, J. Electrochem. Soc. **110**, 1127 (1963).

⁶D. F. O'Kane and D. R. Mason, J. Electrochem. Soc. **110**, 1132 (1963).

⁷D. Weitze and V. Leute, J. Alloys Compd. **236**, 229 (1996).

⁸M. Zapata-Torres, R. Castro-Rodríguez, A. Zapata-Navarro, J. Mustre de León, and F. J. Espinosa y J. L. Peña, Rev. Mex. Fis. **43**, 429 (1997).

⁹R. Castro-Rodríguez, M. Zapata-Torres, A. Zapata-Navarro, A. I. Oliva, and J. L. Peña, J. Appl. Phys. **79**, 184 (1996).

¹⁰A. Martel, R. Castro-Rodríguez, E. Puron, M. Zapata-Torres, and J. L. Peña, Rev. Mex. Fis. **46**(2), 195 (2000).

¹¹A. C. Larson and R. B. von Dreele, Generalized Structure Analysis System, Document No. LAUR 86-748, Los Alamos National Laboratory, Los Alamos (1993).